Vibrations and Static Responses of Asymmetric Bimorph Disks of Piezoelectric Ceramics

Peter C. Y. Lee, *Member, IEEE*, Rui Huang, *Student Member, IEEE*, Xiaoping Li, and Wei-Heng Shih

Abstract—**In an earlier article, the flexural vibrations in bimorph disks and extensional vibrations in homogeneous disks of piezoelectric ceramics were studied. In the present paper, the coupled flexural and extensional vibrations and static responses in an asymmetric bimorph disk, which is formed by bonding together two piezoelectric ceramic disks of unequal thickness and opposite polarization, are investigated.**

Governing equations of coupled motions for asymmetric bimorphs are deduced from the recently derived 2-D, first-order equations for piezoelectric crystal plates with thickness-graded material properties. Then, closed form solutions of these equations for circular disks are obtained for free vibrations, piezoelectrically forced vibrations, and responses under static voltage difference.

Resonance frequencies, distribution of displacements and surface charges, impedances, and static responses are calculated for asymmetric bimorph disks of various thickness ratios and diameter-to-thickness ratios. Experimental data on resonances and impedances are obtained for asymmetric bimorph disks of PZT-857 for different thickness ratios. Comparisons of predicted and measured results show that the agreements are close.

I. Introduction

When an electric field is applied in the thickness direction, which is parallel to the poling direction of the ceramics, only extensional deformation can be induced in homogeneous plates and flexural deformation in symmetric bimorphs. However, in an asymmetric bimorph, which is formed by bonding together two piezoelectric ceramic plates of different thicknesses and opposite polarization, both the extensional and flexural deformation can be excited, and they are coupled.

Exact solutions of the 3-D equations of linear piezoelectricity for straight-crested waves in symmetric and asymmetric bimorph plates of infinite extent were obtained by Lee and Yu [1] and Lee and Liu [2], respectively. Dispersion relations or frequency vs wave number relations computed from these solutions are useful for accessing the accuracy of approximate 2-D theories. Exact solutions of the 3-D equations for the bimorph, symmetric or asymmetric, of finite extent are extremely difficult to obtain and seem to be unavailable in published works at present.

Manuscript received June 21, 1999; accepted November 17, 1999. This work was supported by Grant No. DAAH 04-95-1-0102 from the U.S. Army Research Office.

P.C.Y. Lee and R. Huang are with the Department of Civil and Environmental Engineering, Princeton University, Princeton, NJ 08544 (e-mail: lee@wave.princeton.edu).

X. Li and W.-H. Shih are with the Department of Materials Engineering, Drexel University, Philadelphia, PA 19104.

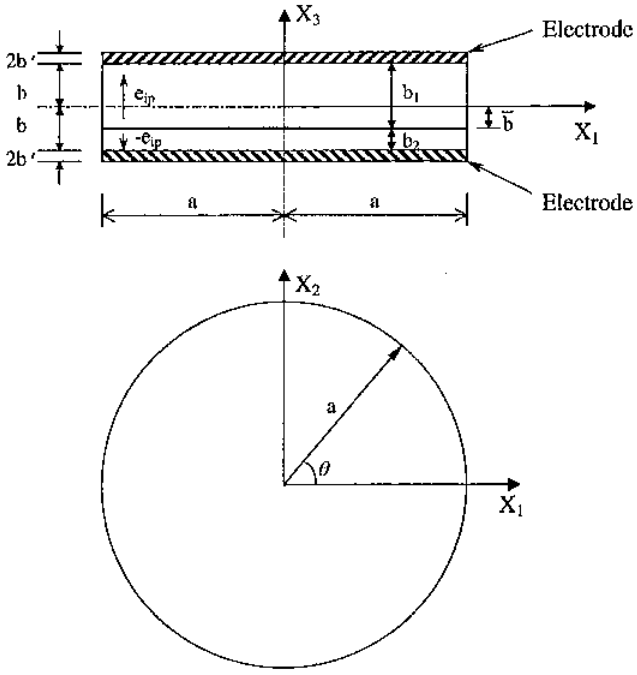

Fig. 1. A circular disk of asymmetric bimorph with electrodes.

Solutions of the approximate 2-D, first-order equations for the extensional and thickness-stretch vibrations for homogeneous disks and flexural and thickness-shear vibrations for symmetric bimorph disks were obtained in [3]. The comparison of computed results with the experimental measurements shows that the agreement is close.

In the present article, governing equations of coupled motions for the asymmetric bimorph plates are deduced from the recently derived 2-D, first-order equations for piezoelectric crystal plates with thickness-graded material properties [1]. Then, closed-form solutions of the equations are obtained for asymmetric bimorph disks for free vibrations, piezoelectrically forced vibrations, and responses under static voltage difference.

Resonance frequencies, distribution of displacements and surface charges, impedances, and static responses are calculated for asymmetric bimorph disks of various thickness ratios and diameter-to-thickness ratios. Experimental data on resonances and impedances are obtained for asymmetric bimorph disks of PZT-857 for different thickness ratios. Comparisons of predicted and measured results show that the agreements are close.

II. 2-D, First-Order Equations

We consider an asymmetric bimorph disk that consists of two ceramic layers of different thicknesses b_1 and b_2 and opposite polarization as shown in Fig. 1. The elastic stiffnesses c_{pq}, dielectric permittivities ϵ_{ij}, and mass density ρ are the same for both layers; the piezoelectric coefficients e_{ip} have the opposite signs:

$$e_{ip}(x_3) = \begin{cases} e_{ip}, & \text{for } b > x_3 > -\bar{b}, \\ -e_{ip}, & \text{for } -\bar{b} > x_3 > -b, \end{cases} \tag{1}$$

where

$$b = \frac{1}{2}(b_1 + b_2), \quad \bar{b} = \frac{1}{2}(b_1 - b_2), \quad r_t = \frac{b_2}{b_1}, \tag{2}$$

ρ' is the density, and $2b'$ is the thickness of the identical electrodes.

The 2-D, first-order equations for the asymmetric bimorph plates are deduced from the general equations for piezoelectric crystal plates with graded material properties across the thickness in [1]. By using the symmetry of material constants of ceramics and considering only the mass effect of electrodes, the equations of [1] are reduced as follows:

$$\begin{aligned} &u_j(x_1, x_2, x_3, t) = u_j^{(0)}(x_1, x_2, t) + x_3 u_j^{(1)}(x_1, x_2, t), \\ &\quad j = 1, 2, 3, \\ &\phi(x_1, x_2, x_3, t) = \bar{V}_0 + \tfrac{x_3}{b}\bar{V}_1 + (1 - \tfrac{x_3^2}{b^2})[\phi^{(0)}(x_1, x_2, t) \\ &\quad + x_3\phi^{(1)}(x_1, x_2, t)], \end{aligned} \tag{3}$$

and [see (4); top of next page] where [see (5); top of next page] and

$$\begin{aligned} \tilde{c}_{11}^{(0)} &= c_{11} - \tfrac{c_{13}^2}{c_{33}}, & \tilde{c}_{12}^{(0)} &= c_{12} - \tfrac{c_{13}^2}{c_{33}}, \\ \tilde{e}_{31}^{(0)} &= \bar{e}_{31}^{(0)} - \tfrac{c_{13}c_{33}^{(0)}}{c_{33}}, & \tilde{\epsilon}_{33}^{(0)} &= \epsilon_{33} + \tfrac{\bar{e}_{33}^{(0)2}}{c_{33}}, \\ \tilde{e}_{31}^{(1)} &= \bar{e}_{31}^{(1)} - \tfrac{c_{13}c_{33}^{(1)}}{c_{33}}, & \tilde{e}_{31}^{(3)} &= \bar{e}_{31}^{(3)} - \tfrac{c_{13}\bar{e}_{33}^{(3)}}{c_{33}}, \\ \tilde{\epsilon}_{33}^{(3)} &= \tfrac{\bar{e}_{33}^{(0)}\bar{e}_{33}^{(3)}}{c_{33}}, & \hat{\epsilon}_{33}^{(1)} &= \tfrac{\bar{e}_{33}^{(1)}\bar{e}_{33}^{(0)}}{c_{33}}, \\ \hat{\epsilon}_{33}^{(0)} &= \epsilon_{33} - \tfrac{b^2\bar{e}_{33}^{(1)2}}{3c_{33}}, & \hat{\epsilon}_{33}^{(2)} &= \epsilon_{33} + \tfrac{3b^2\bar{e}_{33}^{(1)}\bar{e}_{33}^{(3)}}{5c_{33}}, \\ \hat{\epsilon}_{33}^{(4)} &= \epsilon_{33} + \tfrac{3b^2\bar{e}_{33}^{(3)2}}{5c_{33}}. \end{aligned} \tag{6}$$

We note that $\kappa_4 = \kappa_5$ has been employed in (4) because ceramics are transversely isotropic in the plane perpendicular to the poling axis x_3.

In (4), the symmetric and antisymmetric motions with respect to the middle plane are coupled together. The coupling comes from the modified piezoelectric coefficients $\bar{e}_{ip}^{(n)}$, which depend on the thickness gradient of $e_{ip}(x_3)$. For an asymmetric bimorph plate, as shown in Fig. 1 and given by (1), $e_{ip}(x_3)$ has a discontinuity at the interface of two layers, i.e., at $x_3 = -\bar{b}$. The modified coefficients $\bar{e}_{ip}^{(n)}$ are determined in a manner slightly simpler than that employed in [1]. By substituting the 3-D stress-strain relations $T_p = c_{pq}S_q - e_{ip}E_i$ into the definition of the nth order stress component, we have

$$T_p^{(n)} = \int_{-b}^{b} x_3^n \left(c_{pq}S_q - e_{ip}E_i\right) dx_3 \tag{7}$$

in which the strain S_q and electric field E_i for the first-order approximation are given by

$$\begin{aligned} S_q &= S_q^{(0)} + x_3 S_q^{(1)}, \\ E_i &= E_i^{(0)} + x_3 E_i^{(1)} + x_3^2 E_i^{(2)} + x_3^3 E_i^{(3)}. \end{aligned} \tag{8}$$

By inserting (8) into (7), separating the integration into two intervals, i.e., from $-b$ to $-\bar{b}$ and from $-\bar{b}$ to b, and taking (1) into account, we obtain

$$\begin{aligned} T_p^{(0)} =& 2b\left(c_{pq}S_q^{(0)} - \frac{\bar{b}}{b}e_{kp}E_k^{(0)} - \frac{\bar{b}^3}{3b}e_{kp}E_k^{(2)}\right) \\ &- \frac{2b^3}{3}\left[\frac{3}{2b}(1 - \frac{\bar{b}^2}{b^2})e_{kp}E_k^{(1)} + \frac{3b}{4}(1 - \frac{\bar{b}^4}{b^4})e_{kp}E_k^{(3)}\right], \\ T_p^{(1)} =& \frac{2b^3}{3}\left[c_{pq}S_q^{(1)} - \frac{3}{2b}(1 - \frac{\bar{b}^2}{b^2})e_{kp}E_k^{(0)} - \frac{\bar{b}^3}{b^3}e_{kp}E_k^{(1)}\right. \\ &\left. - \frac{3b}{4}(1 - \frac{\bar{b}^4}{b^4})e_{kp}E_k^{(2)} - \frac{3\bar{b}^5}{5b^3}e_{kp}E_k^{(3)}\right]. \end{aligned} \tag{9}$$

Comparison of the above relationships with the 2-D constitutive equations (83) of [1], rewritten in the following manner:

$$\begin{aligned} T_p^{(0)} =& 2b\left(c_{pq}S_q^{(0)} - \bar{e}_{kp}E_k^{(0)} - \frac{b^2}{3}\bar{e}_{kp}^{(0)}E_k^{(2)}\right) \\ &- \frac{2b^3}{3}\left(\bar{e}_{kp}^{(1)}E_k^{(1)} - \frac{3b^2}{5}\bar{e}_{kp}^{(3)}E_k^{(3)}\right), \\ T_p^{(1)} =& \frac{2b^3}{3}\left(c_{pq}S_q^{(1)} - \bar{e}_{kp}^{(1)}E_k^{(0)} - \bar{e}_{kp}^{(0)}E_k^{(1)}\right. \\ &\left. - \frac{3b^2}{5}\bar{e}_{kp}^{(3)}E_k^{(2)} - \frac{3b^2}{5}\bar{3}_{kp}^{(2)}E_k^{(3)}\right), \end{aligned} \tag{10}$$

leads to

$$\begin{aligned} &\bar{e}_{kp} = \tfrac{\bar{b}}{b}e_{kp}, \quad \bar{e}_{kp}^{(0)} = \tfrac{\bar{b}^3}{b^3}e_{kp}, \quad \bar{e}_{kp}^{(2)} = \tfrac{b^5}{b^5}e_{kp}, \\ &b\bar{e}_{kp}^{(1)} = \tfrac{3}{2}(1 - \tfrac{\bar{b}^2}{b^2})e_{kp}, \; b\bar{e}_{kp}^{(3)} = \tfrac{5}{4}(1 - \tfrac{\bar{b}^4}{b^4})e_{kp}. \end{aligned} \tag{11}$$

We note that (4) is coupled through the coefficients in (11). By letting $\bar{b} = b$ or $\bar{b} = 0$ in (11), (4) can be reduced to the uncoupled cases for the homogeneous plate or symmetric bimorph plate, respectively, as they were studied in [1], [3].

For traction-free and charge-free edge conditions, according to (77) of [1], we require

$$t_{rr}^{(n)} = t_{r\theta}^{(n)} = t_{rz}^{(n)} = D_r^{(n)*} = 0, \quad n = 0, 1 \quad \text{at } r = a. \tag{12}$$

The components of tractions and charges in (12) are related to the displacements $u_j^{(n)}$ and electric potentials

$$
\begin{aligned}
&\tfrac{c_{11}+c_{12}}{2}\nabla(\nabla\cdot\mathbf{u}_T^{(0)})+c_{66}\nabla^2\mathbf{u}_T^{(0)}+\kappa_3 c_{13}\nabla u_3^{(1)}-\tfrac{2}{3}\bar{e}_{31}^{(1)}\nabla\phi^{(0)}\\
&\quad+(\bar{e}_{31}-\bar{e}_{31}^{(0)})\nabla\phi^{(1)}+\tfrac{1}{2b}\mathbf{F}_T^{(0)}=(1+R)\rho\ddot{\mathbf{u}}_T^{(0)},\\
&\kappa_5^2 c_{55}(\nabla^2 u_3^{(0)}+\nabla\cdot\mathbf{u}_T^{(1)})+\kappa_5(\bar{e}_{15}-\tfrac{1}{3}\bar{e}_{15}^{(0)})\nabla^2\phi^{(0)}+\kappa_5\tfrac{b^2}{3}(\bar{e}_{15}^{(1)}-\tfrac{3}{5}\bar{e}_{15}^{(3)})\nabla^2\phi^{(1)}\\
&\quad+\tfrac{1}{2b}\mathcal{F}_3^{(0)}=(1+R)\rho\ddot{u}_3^{(0)},\\
&\tfrac{\bar{c}_{11}^{(0)}+\bar{c}_{12}^{(0)}}{2}\nabla(\nabla\cdot\mathbf{u}_T^{(1)})+c_{66}\nabla^2\mathbf{u}_T^{(1)}-\tfrac{2}{b^2}[\tilde{e}_{31}^{(0)}+\tfrac{3}{2}\kappa_5(\bar{e}_{15}-\tfrac{1}{3}\bar{e}_{15}^{(0)})]\nabla\phi^{(0)}\\
&\quad-\tfrac{3}{b^2}\kappa_5^2 c_{55}(\nabla u_3^{(0)}+\mathbf{u}_T^{(1)})+[\tilde{e}_{31}^{(1)}-\tfrac{9}{5}\tilde{e}_{31}^{(3)}-\kappa_5(\bar{e}_{15}^{(1)}-\tfrac{3}{5}\bar{e}_{15}^{(3)})]\nabla\phi^{(1)}\\
&\quad+\tfrac{3}{2b^3}\mathbf{F}_T^{(1)}=(1+3R)\rho\ddot{\mathbf{u}}_T^{(1)},\\
&c_{55}\nabla^2 u_3^{(1)}-\tfrac{3}{b^2}\kappa_3(c_{13}\nabla\cdot\mathbf{u}_T^{(0)}+\kappa_3 c_{33}u_3^{(1)})+(e_{15}^{(0)}-\tfrac{3}{5}\bar{e}_{15}^{(2)})\nabla^2\phi^{(1)}\\
&\quad-\tfrac{3}{b^2}\kappa_3(\bar{e}_{33}-\bar{e}_{33}^{(0)})\phi^{(1)}+(\bar{e}_{15}^{(1)}-\tfrac{3}{5}\bar{e}_{15}^{(3)})\nabla^2\phi^{(0)}\\
&\quad+\tfrac{2}{b^2}\kappa_3\bar{e}_{33}^{(1)}\phi^{(0)}-\tfrac{3}{b^3}\kappa_3\bar{c}_{33}\bar{V}_1+\tfrac{3}{2b^3}\mathcal{F}_3^{(1)}=(1+3R)\rho\ddot{u}_3^{(1)},\\
&\kappa_5(\bar{e}_{15}-\tfrac{1}{3}\bar{e}_{15}^{(0)})(\nabla^2 u_3^{(0)}+\nabla\cdot\mathbf{u}_T^{(1)})+\tfrac{2}{3}\bar{e}_{31}^{(0)}\nabla\cdot\mathbf{u}_T^{(1)}+\tfrac{b^2}{3}(e_{15}^{(1)}-\tfrac{3}{5}\bar{e}_{15}^{(3)})\nabla^2 u_3^{(1)}\\
&\quad+\tfrac{2}{3}\kappa_3\bar{e}_{33}^{(1)}u_3^{(1)}+\tfrac{2}{3}\bar{e}_{31}^{(1)}\nabla\cdot\mathbf{u}_T^{(0)}-\tfrac{8}{15}\epsilon_{11}\nabla^2\phi^{(0)}\\
&\quad+\tfrac{4}{3b^2}\hat{e}_{33}^{(0)}\phi^{(0)}-\tfrac{2}{3}(\hat{e}_{33}^{(1)}-\tfrac{9}{5}\hat{e}_{33}^{(3)})\phi^{(1)}-\tfrac{2}{3b}\hat{e}_{33}^{(1)}\bar{V}_1=0,\\
&\kappa_5(\bar{e}_{15}^{(1)}-\tfrac{3}{5}\bar{e}_{15}^{(3)})\nabla^2 u_3^{(0)}+(\bar{e}_{15}^{(0)}-\tfrac{3}{5}\bar{e}_{15}^{(2)})\nabla^2 u_3^{(1)}-\tfrac{3}{b^2}(\bar{e}_{31}-\bar{c}_{31}^{(0)})\nabla\cdot\mathbf{u}_T^{(0)}\\
&\quad-\tfrac{3}{b^2}\kappa_3(\bar{e}_{33}-\bar{c}_{33}^{(0)})u_3^{(1)}+[\kappa_5(\bar{e}_{15}^{(1)}-\tfrac{3}{5}\bar{e}_{15}^{(3)})-(\tilde{e}_{31}^{(1)}-\tfrac{9}{5}\tilde{e}_{31}^{(3)})]\nabla\cdot\mathbf{u}_T^{(1)}\\
&\quad-\tfrac{8}{35}\epsilon_{11}\nabla^2\phi^{(1)}+\tfrac{3}{b^2}(\hat{e}_{33}^{(0)}-2\hat{e}_{33}^{(2)}+\tfrac{9}{5}\hat{e}_{33}^{(4)})\phi^{(1)}\\
&\quad-\tfrac{2}{b^2}(\hat{e}_{33}^{(1)}-\tfrac{9}{5}\hat{e}_{33}^{(3)})\phi^{(0)}+(\hat{e}_{33}^{(0)}-\hat{e}_{33}^{(2)})\tfrac{3\bar{V}_1}{b^3}=0,
\end{aligned}
\tag{4}
$$

$$
\begin{aligned}
&\mathbf{u}_T^{(0)}=u_1^{(0)}\mathbf{c}_1+u_2^{(0)}\mathbf{e}_2, && \mathbf{u}_T^{(1)}=u_1^{(1)}\mathbf{c}_1+u_2^{(1)}\mathbf{e}_2,\\
&\mathbf{F}_T^{(0)}=\mathcal{F}_1^{(0)}\mathbf{c}_1+\mathcal{F}_2^{(0)}\mathbf{e}_2, && \mathbf{F}_T^{(1)}=\mathcal{F}_1^{(1)}\mathbf{e}_1+\mathcal{F}_2^{(1)}\mathbf{e}_2,\\
&\mathcal{F}_j^{(n)}=b^n\left[I_{3j}(B)-(-1)^n T_{3j}(-B)\right], && B=b+2b', j=1,2,3,\ n=0,1,\\
&\nabla=\mathbf{c}_1\tfrac{\partial}{\partial x_1}+\mathbf{e}_2\tfrac{\partial}{\partial x_2}, && R=\tfrac{2\rho' b'}{\rho b},
\end{aligned}
\tag{5}
$$

$\phi^{(n)}$ by the following constitutive equations:

$$
\begin{aligned}
t_{rr}^{(0)}&=2b\left[c_{12}\nabla\cdot\mathbf{u}_T^{(0)}+2c_{66}\tfrac{\partial u_r^{(0)}}{\partial r}+\kappa_3 c_{13}u_3^{(1)}\right.\\
&\quad\left.-\tfrac{2}{3}\bar{e}_{31}^{(1)}\phi^{(0)}+(\bar{e}_{31}-\bar{e}_{31}^{(0)})\phi^{(1)}\right]+2\bar{e}_{31}\bar{V}_1,\\
t_{r\theta}^{(0)}&=2bc_{66}\left(\tfrac{\partial u_\theta^{(0)}}{\partial r}-\tfrac{u_\theta^{(0)}}{r}+\tfrac{1}{r}\tfrac{\partial u_r^{(0)}}{\partial\theta}\right),\\
t_{rr}^{(1)}&=\tfrac{2b^3}{3}\left[2c_{66}\tfrac{\partial u_r^{(1)}}{\partial r}+\tilde{c}_{12}^{(0)}\nabla\cdot\mathbf{u}_T^{(1)}-\tfrac{2}{b^2}\tilde{e}_{31}^{(0)}\phi^{(0)}\right.\\
&\quad\left.+(\tilde{e}_{31}^{(1)}-\tfrac{9}{5}\tilde{e}_{31}^{(3)})\phi^{(1)}+\tilde{e}_{31}^{(1)}\tfrac{\bar{V}_1}{b}\right],\\
t_{r\theta}^{(1)}&=\tfrac{2b^3}{3}c_{66}\left(\tfrac{\partial u_\theta^{(1)}}{\partial r}-\tfrac{u_\theta^{(1)}}{r}+\tfrac{1}{r}\tfrac{\partial u_r^{(1)}}{\partial\theta}\right),\\
t_{rz}^{(0)}&=2b\kappa_5\left[\kappa_5 c_{55}\left(\tfrac{\partial u_3^{(0)}}{\partial r}+u_r^{(1)}\right)+(\bar{e}_{15}-\tfrac{1}{3}\bar{e}_{15}^{(0)})\right.\\
&\quad\left.\tfrac{\partial\phi^{(0)}}{\partial r}+\tfrac{b^2}{3}(\bar{e}_{15}^{(1)}-\tfrac{3}{5}\bar{e}_{15}^{(3)})\tfrac{\partial\phi^{(1)}}{\partial r}\right],\\
t_{rz}^{(1)}&=\tfrac{2b^3}{3}\left[c_{55}\tfrac{\partial u_3^{(1)}}{\partial r}+(\bar{e}_{15}^{(1)}-\tfrac{3}{5}\bar{e}_{15}^{(3)})\tfrac{\partial\phi^{(0)}}{\partial r}\right.\\
&\quad\left.+(\bar{e}_{15}^{(0)}-\tfrac{3}{5}\bar{e}_{15}^{(2)})\tfrac{\partial\phi^{(1)}}{\partial r}\right],\\
D_r^{(0)*}&=2b\left[\kappa_5(\bar{e}_{15}-\tfrac{1}{3}\bar{e}_{15}^{(0)})\left(\tfrac{\partial u_3^{(0)}}{\partial r}+u_r^{(1)}\right)\right.\\
&\quad\left.+\tfrac{b^2}{3}(\bar{e}_{15}^{(1)}-\tfrac{3}{5}\bar{e}_{15}^{(3)})\tfrac{\partial u_3^{(1)}}{\partial r}-\tfrac{8}{15}\epsilon_{11}\tfrac{\partial\phi^{(0)}}{\partial r}\right],\\
D_r^{(1)*}&=\tfrac{2b^3}{3}\left[\kappa_5(\bar{e}_{15}^{(1)}-\tfrac{3}{5}\bar{e}_{15}^{(3)})\left(\tfrac{\partial u_3^{(0)}}{\partial r}+u_r^{(1)}\right)\right.\\
&\quad\left.+(\bar{e}_{15}^{(0)}-\tfrac{3}{5}\bar{e}_{15}^{(2)})\tfrac{\partial u_3^{(1)}}{\partial r}-\tfrac{8}{35}\epsilon_{11}\tfrac{\partial\phi^{(1)}}{\partial r}\right].
\end{aligned}
\tag{13}
$$

III. Free Vibrations

In this section, the first-order, 2-D equations (4) are solved for closed-form solutions of free vibrations of asymmetric bimorph disks of ceramics.

By taking the divergence of $(4)_{1,3}$, setting $\mathbf{F}_T^{(0)}$, $\mathbf{F}_T^{(1)}$, $\mathcal{F}_3^{(0)}$, $\mathcal{F}_3^{(1)}$, $\bar{V}_1$ to zero for free vibrations with shorted electrodes and using the relation $c_{11}-c_{12}=\tilde{c}_{11}^{(0)}-\tilde{c}_{12}^{(0)}=2c_{66}$, we have

$$
\begin{aligned}
&c_{11}\nabla^2(\nabla\cdot\mathbf{u}_T^{(0)})+\kappa_3 c_{13}\nabla^2 u_3^{(1)}-\tfrac{2}{3}\bar{e}_{31}^{(1)}\nabla^2\phi^{(0)}\\
&\quad+(\bar{e}_{31}-\bar{e}_{31}^{(0)})\nabla^2\phi^{(1)}=(1+R)\rho\nabla\cdot\ddot{\mathbf{u}}_T^{(0)},\\
&\tilde{c}_{11}^{(0)}\nabla^2(\nabla\cdot\mathbf{u}_T^{(1)})-\tfrac{3\kappa_5^2 c_{55}}{b^2}\left(\nabla^2 u_3^{(0)}+\nabla\cdot\mathbf{u}_T^{(1)}\right)\\
&\quad-\tfrac{2}{b^2}\left[\tilde{e}_{31}^{(0)}+\tfrac{3}{2}\kappa_5(\bar{e}_{15}-\tfrac{1}{3}\bar{e}_{15}^{(0)})\right]\nabla^2\phi^{(0)}\\
&\quad+\left[\tilde{e}_{31}^{(1)}-\tfrac{9}{5}\tilde{e}_{31}^{(3)}-\kappa_5\left(\bar{e}_{15}^{(1)}-\tfrac{3}{5}\bar{e}_{15}^{(3)}\right)\right]\nabla^2\phi^{(1)}\\
&\quad=(1+3R)\rho\nabla\cdot\ddot{\mathbf{u}}_T^{(1)}.
\end{aligned}
\tag{14}
$$

For axisymmetric vibrations of a circular disk, we let

$$
\begin{aligned}
\nabla\cdot\mathbf{u}_T^{(0)}&=A_1 J_0(\xi r)e^{i\omega t},\\
u_3^{(0)}&=bA_2 J_0(\xi r)e^{i\omega t},\\
\nabla\cdot\mathbf{u}_T^{(1)}&=\tfrac{1}{b}A_3 J_0(\xi r)e^{i\omega t},
\end{aligned}
$$

$$
\begin{aligned}
u_3^{(1)} &= A_4 J_0(\xi r) e^{i\omega t},\\
\phi^{(0)} &= bA_5\sqrt{\tfrac{c_{55}}{\epsilon_{33}}} J_0(\xi r) e^{i\omega t},\\
\phi^{(1)} &= A_6\sqrt{\tfrac{c_{55}}{\epsilon_{33}}} J_0(\xi r) e^{i\omega t}.
\end{aligned}
\tag{15}
$$

Upon substituting (15) into (14) and $(4)_{2,4,5,6}$, we obtain

$$
\sum_{j=1}^{6} Q_{ij}(X;\Omega) A_j = 0, \quad i = 1, 2, \cdots, 6 \tag{16}
$$

where the elements of the matrix are

$$
\begin{aligned}
Q_{11} &= R_1\Omega^2 - \frac{c_{11}}{c_{55}}X^2,\\
Q_{22} &= R_1\Omega^2 - \kappa_5^2 X^2,\\
Q_{33} &= \frac{\pi^2}{12}\left(R_2\Omega^2 - \frac{\tilde{c}_{11}^{(0)}}{c_{55}}X^2\right) - \kappa_5^2,\\
Q_{44} &= \frac{\pi^2}{12}\left(R_2\Omega^2 - X^2\right) - \kappa_3^2\frac{c_{33}}{c_{55}},\\
Q_{55} &= \frac{4\tilde{\epsilon}_{33}^{(0)}}{3\epsilon_{33}} + \frac{2\pi^2}{15}\frac{c_{11}}{\epsilon_{33}}X^2,\\
Q_{66} &= \frac{\hat{\epsilon}_{33}^{(6)}}{\epsilon_{33}} + \frac{2\pi^2}{105}\frac{\epsilon_{11}}{\epsilon_{33}}X^2,\\
Q_{14} &= Q_{41}X^2 = -\kappa_3\frac{c_{13}}{c_{55}}X^2,\\
Q_{15} &= Q_{51}X^2 = \frac{2}{3}\frac{b\bar{e}_{31}^{(1)}}{\sqrt{c_{55}\epsilon_{33}}}X^2,\\
Q_{16} &= Q_{61}X^2 = -\frac{\bar{e}_{31}^{(4)}}{\sqrt{c_{55}\epsilon_{33}}}X^2,\\
Q_{32} &= \frac{\pi^4}{16}X^2 Q_{23} = \frac{\pi^2}{4}\kappa_5^2 X^2,\\
Q_{52} &= \frac{\pi^2}{4}Q_{25} = \kappa_5\frac{\pi^2}{4}\frac{\bar{e}_{15}^{(4)}}{\sqrt{c_{55}\epsilon_{33}}}X^2,\\
Q_{62} &= \frac{\pi^2}{4}Q_{26} = -\kappa_5\frac{\pi^2}{12}\frac{b\bar{e}_{15}^{(5)}}{\sqrt{c_{55}\epsilon_{33}}}X^2,\\
Q_{35} &= \frac{\pi^2}{4}X^2 Q_{53} = \frac{\pi^2}{4}\frac{\kappa_5\tilde{e}_{15}^{(4)} + \frac{2}{3}\tilde{e}_{31}^{(0)}}{\sqrt{c_{55}\epsilon_{33}}}X^2,\\
Q_{36} &= \frac{\pi^2}{4}X^2 Q_{63} = \frac{\pi^2}{12}\frac{b(\kappa_5\tilde{e}_{15}^{(5)} - \tilde{e}_{31}^{(5)})}{\sqrt{c_{55}\epsilon_{33}}}X^2,\\
Q_{45} &= Q_{54} = \frac{2}{3}\frac{b(\kappa_3\bar{e}_{31}^{(1)} - \frac{\pi^2}{8}\bar{e}_{15}^{(5)}X^2)}{\sqrt{c_{55}\epsilon_{33}}},\\
Q_{46} &= Q_{64} = -\frac{\kappa_3\bar{e}_{33}^{(4)} + \frac{\pi^2}{12}\bar{e}_{15}^{(6)}X^2}{\sqrt{c_{55}\epsilon_{33}}},\\
Q_{56} &= Q_{65} = -\frac{2b\hat{e}_{33}^{(5)}}{3\epsilon_{33}},\\
Q_{12} &= Q_{13} = Q_{21} = Q_{31} = Q_{24} = Q_{34} = Q_{42} = Q_{43} = 0,
\end{aligned}
\tag{17}
$$

and

$$
\begin{aligned}
&X = \tfrac{2\xi b}{\pi}, && \Omega = \tfrac{2\omega b}{\pi}\sqrt{\tfrac{\rho}{c_{55}}},\\
&R_1 = 1 + R, && R_2 = 1 + 3R,\\
&\bar{e}_{31}^{(4)} = \bar{e}_{31} - \bar{e}_{31}^{(0)}, && \bar{e}_{33}^{(4)} = \bar{e}_{33} - \bar{e}_{33}^{(0)},\\
&\bar{e}_{15}^{(4)} = \bar{e}_{15} - \tfrac{1}{3}\bar{e}_{15}^{(0)}, && \bar{e}_{15}^{(5)} = \bar{e}_{15}^{(1)} - \tfrac{3}{5}\bar{e}_{15}^{(3)},\\
&\bar{e}_{15}^{(6)} = \bar{e}_{15}^{(0)} - \tfrac{3}{5}\bar{e}_{15}^{(2)}, && \bar{e}_{31}^{(5)} = \bar{e}_{31}^{(1)} - \tfrac{9}{5}\tilde{e}_{31}^{(3)},\\
&\hat{e}_{33}^{(5)} = \hat{e}_{33}^{(1)} - \tfrac{9}{5}\tilde{e}_{33}^{(3)}), && \hat{e}_{33}^{(6)} = \hat{e}_{33}^{(0)} - 2\hat{e}_{33}^{(2)} + \tfrac{9}{5}\hat{e}_{33}^{(4)}.
\end{aligned}
\tag{18}
$$

For nontrivial solutions to (16), we have

$$
\det[Q_{ij}(X;\Omega)] = 0, \tag{19}
$$

which gives the dispersion relations for the free vibrations of an infinite bimorph disk. By letting $X = 0$ in (19), we obtain two cut-off frequencies:

$$
\Omega_{c1} = \kappa_5\tfrac{2}{\pi}\sqrt{\tfrac{3}{1+3R}}, \quad \Omega_{c2} = \kappa_3\tfrac{2}{\pi}\sqrt{\tfrac{3A}{(1+3R)B}} \tag{20}
$$

where

$$
A = \begin{vmatrix}
-\frac{c_{33}}{c_{55}} & \frac{b\bar{e}_{33}^{(1)}}{\sqrt{c_{55}c_{33}}} & -\frac{e_{33}^{(4)}}{\sqrt{c_{55}c_{33}}}\\
\frac{bc_{33}^{(1)}}{\sqrt{c_{55}c_{33}}} & \frac{3\tilde{c}_{33}^{(0)}}{c_{33}} & -\frac{b\tilde{e}_{33}^{(5)}}{c_{33}}\\
-\frac{\bar{e}_{33}^{(4)}}{\sqrt{c_{55}c_{33}}} & -\frac{b\hat{e}_{33}^{(5)}}{c_{33}} & \frac{\hat{e}_{33}^{(6)}}{\epsilon_{33}}
\end{vmatrix}, \tag{21}
$$

$$
B = \tfrac{b^2\hat{e}_{33}^{(5)2}}{c_{33}^2} - \tfrac{3\tilde{c}_{33}^{(0)}\hat{e}_{33}^{(6)}}{\epsilon_{33}^2}.
$$

The correction factors κ_3, κ_5 in 2-D equations are obtained by equating Ω_{c1} and Ω_{c2}, respectively, to the frequencies of simple (slow) thickness-shear mode and simple thickness-stretch mode of the 3-D equations given in the Appendix. The dispersion curves are calculated for a bimorph disk of PZT-857 with thickness ratio $r_t = 0.127$ and plotted in Fig. 2. The values of material constants of PZT-857 for calculations were given in [3].

We note that (19) is a sixth-order equation of X^2. For a given value of Ω, this equation has six roots: X_j or ξ_j, $j = 1, \cdots, 6$. All of these roots are needed for the general solutions to satisfy the edge condition (12). Hence, we let

$$
\begin{aligned}
\nabla\cdot\mathbf{u}_T^{(0)} &= \sum_{j=1}^{6}\alpha_{1j}B_j J_0(\xi_j r)e^{i\omega t},\\
u_3^{(0)} &= b\sum_{j=1}^{6}\alpha_{2j}B_j J_0(\xi_j r)e^{i\omega t},\\
\nabla\cdot\mathbf{u}_T^{(1)} &= \tfrac{1}{b}\sum_{j=1}^{6}\alpha_{3j}B_j J_0(\xi_j r)e^{i\omega t},\\
u_3^{(1)} &= \sum_{j=1}^{6}\alpha_{4j}B_j J_0(\xi_j r)e^{i\omega t},\\
\phi^{(0)} &= b\sqrt{\tfrac{c_{55}}{\epsilon_{33}}}\sum_{j=1}^{6}\alpha_{5j}B_j J_0(\xi_j r)e^{i\omega t},\\
\phi^{(1)} &= \sqrt{\tfrac{c_{55}}{\epsilon_{33}}}\sum_{j=1}^{6}\alpha_{6j}B_j J_0(\xi_j r)e^{i\omega t}
\end{aligned}
\tag{22}
$$

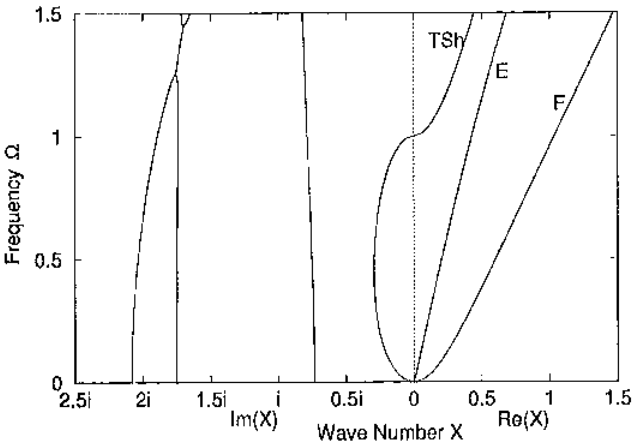

Fig. 2. Dispersion curves of coupled flexural and extensional vibrations for asymmetric bimorph plates of PZT-857 ($b_1 = 0.100$ cm; $b_2 = 0.0127$ cm).

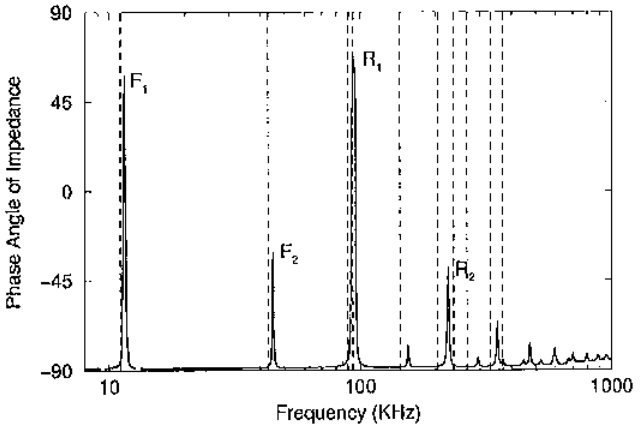

Fig. 3. Comparison of computed resonance frequencies (dashed lines) of coupled flexural and extensional vibrations with the measured phase angle of impedance (solid lines) for the asymmetric bimorph disk of PZT-857 with $a = 1.27$ cm, and $b_1 = 0.100$ cm, $b_2 = 0.0127$ cm.

where the ratios of the amplitudes, α_{ij}, satisfy

$$\sum_{k=1}^{6} Q_{ik}(X_j;\Omega)\alpha_{kj} = 0, \quad i,j = 1,2,\cdots,6. \tag{23}$$

For axisymmetric vibrations of a circular disk, we have $\nabla^2 \mathbf{u}_T^{(n)} = \nabla\left(\nabla \cdot \mathbf{u}_T^{(n)}\right)$ for $n = 0, 1$. Thus, by solving $(4)_{1,3}$ and, again, noting that $c_{11} - c_{12} = \tilde{c}_{11}^{(0)} - \tilde{c}_{12}^{(0)} = 2c_{66}$, we obtain the components of the radial displacement:

$$\begin{aligned} u_r^{(0)} &= -\tfrac{4b^2}{\pi^2(1+R)\Omega^2}\tfrac{\partial}{\partial r} \\ &\quad \left[\tfrac{c_{11}}{c_{55}}\nabla\cdot\mathbf{u}_T^{(0)} + \kappa_3\tfrac{c_{13}}{c_{55}}u_3^{(1)} - \tfrac{2\tilde{e}_{31}^{(1)}}{3c_{55}}\phi^{(0)} + \tfrac{\tilde{e}_{31}^{(4)}}{c_{55}}\phi^{(1)}\right], \\ u_r^{(1)} &= \tfrac{4}{\pi^2\lambda}\tfrac{\partial}{\partial r}\left[3\kappa_5^2 u_3^{(0)} - \tfrac{\tilde{e}_{11}^{(0)}}{c_{55}}b^2\nabla\cdot\mathbf{u}_T^{(1)} + \right. \\ &\quad \left. \tfrac{2\tilde{e}_{31}^{(0)}+3\kappa_5\tilde{e}_{15}^{(4)}}{c_{55}}\phi^{(0)} - \tfrac{b^2(\tilde{e}_{31}^{(5)}-\kappa_5\tilde{e}_{15}^{(1)})}{c_{55}}\phi^{(1)}\right] \end{aligned} \tag{24}$$

where

$$\lambda = (1+3R)\Omega^2 - \frac{12}{\pi^2}\kappa_5^2. \tag{25}$$

Substituting (22) into (24), we have

$$\begin{aligned} u_r^{(0)} &= \tfrac{2b}{\pi(1+R)\Omega^2}\textstyle\sum_{j=1}^{6}\beta_{1j}X_jB_jJ_1(\xi_j r)e^{i\omega t}, \\ u_r^{(1)} &= \tfrac{2}{\pi\lambda}\textstyle\sum_{j=1}^{6}\beta_{2j}X_jB_jJ_1(\xi_j r)e^{i\omega t} \end{aligned} \tag{26}$$

where

$$\begin{aligned} &\beta_{1j} = \\ &\tfrac{c_{11}}{c_{55}}\alpha_{1j} + \kappa_3\tfrac{c_{13}}{c_{55}}\alpha_{4j} - \tfrac{2b\tilde{e}_{31}^{(1)}}{3\sqrt{c_{55}\epsilon_{33}}}\alpha_{5j} + \tfrac{\tilde{e}_{31}^{(4)}}{\sqrt{c_{55}\epsilon_{33}}}\alpha_{6j}, \\ &\beta_{2j} = \\ &-3\kappa_5^2\alpha_{2j} + \tfrac{\tilde{e}_{11}^{(0)}}{c_{55}}\alpha_{3j} - \tfrac{2\tilde{e}_{31}^{(0)}+3\kappa_5\tilde{e}_{15}^{(4)}}{\sqrt{c_{55}\epsilon_{33}}}\alpha_{5j} + \tfrac{b(\tilde{e}_{31}^{(5)}-\kappa_5\tilde{e}_{15}^{(5)})}{\sqrt{c_{55}\epsilon_{33}}}\alpha_{6j}. \end{aligned} \tag{27}$$

The requirement of (22) and (26) to satisfy the free edge condition (12) leads to

$$\sum_{j=1}^{6} M_{ij}B_j = 0, \quad i = 1,\cdots,6 \tag{28}$$

where the coefficients are defined by

$$\begin{aligned} M_{1j} &= \tfrac{c_{66}}{c_{55}}\left[-2\alpha_{1j} + \left(\tfrac{c_{55}}{c_{66}} + \tfrac{2X_j^2}{(1+R)\Omega^2}\right)\beta_{1j}\right]J_0(\xi_j a) \\ &\quad - \tfrac{c_{66}}{c_{55}}\tfrac{2X_j^2\beta_{1j}}{(1+R)\Omega^2}\tfrac{J_1(\xi_j a)}{\xi_j a}, \\ M_{2j} &= \left[\tfrac{2c_{66}}{\lambda c_{55}}\beta_{2j}X_j^2 + \tfrac{\tilde{c}_{12}^{(0)}}{c_{55}}\alpha_{3j} - \tfrac{2\tilde{e}_{31}^{(0)}}{\sqrt{c_{55}\epsilon_{33}}}\alpha_{5j} + \tfrac{b\tilde{e}_{31}^{(5)}}{\sqrt{c_{55}\epsilon_{33}}}\alpha_{6j}\right] \\ &\quad J_0(\xi_j a) - \tfrac{2c_{66}}{\lambda c_{55}}\beta_{2j}X_j^2\tfrac{J_1(\xi_j a)}{\xi_j a}, \\ M_{3j} &= \left(-\lambda\alpha_{2j} + \tfrac{4}{\pi^2}\beta_{2j}\right)X_jJ_1(\xi_j a), \\ M_{4j} &= \alpha_{4j}X_jJ_1(\xi_j a), \\ M_{5j} &= \alpha_{5j}X_jJ_1(\xi_j a), \\ M_{6j} &= \alpha_{6j}X_jJ_1(\xi_j a). \end{aligned} \tag{29}$$

The vanishing of the determinant of the coefficient matrix of (28) gives the frequency equation for the free vibrations of the asymmetric bimorph disks.

Experimental measurements are made on asymmetric bimorph disks of PZT-857 with different thickness ratios $r_t = b_2/b_1$. The measured phase angle of impedance vs forcing frequency for the bimorph disk with $d = 2.54$ cm, $b_1 = 0.100$ cm, $b_2 = 0.0127$ cm, and $r_t = 0.127$ is shown by a solid line in Fig. 3. The computed resonance frequencies from (28) for the coupled vibrations are also shown in Fig. 3 by the vertical dashed lines for comparison.

Distributions of displacements and surface charge at the first, second, and fourth resonances in Fig. 3 are computed from (28), (26), and (22); they are shown in Fig. 4, Fig. 5, and Fig. 6, respectively. By examining the relative magnitudes and distributions of the vertical and radial displacements, $u_3^{(0)}$ and $u_r^{(0)}$, these resonances are identified as the fundamental and second flexural modes (F_1 and F_2) and

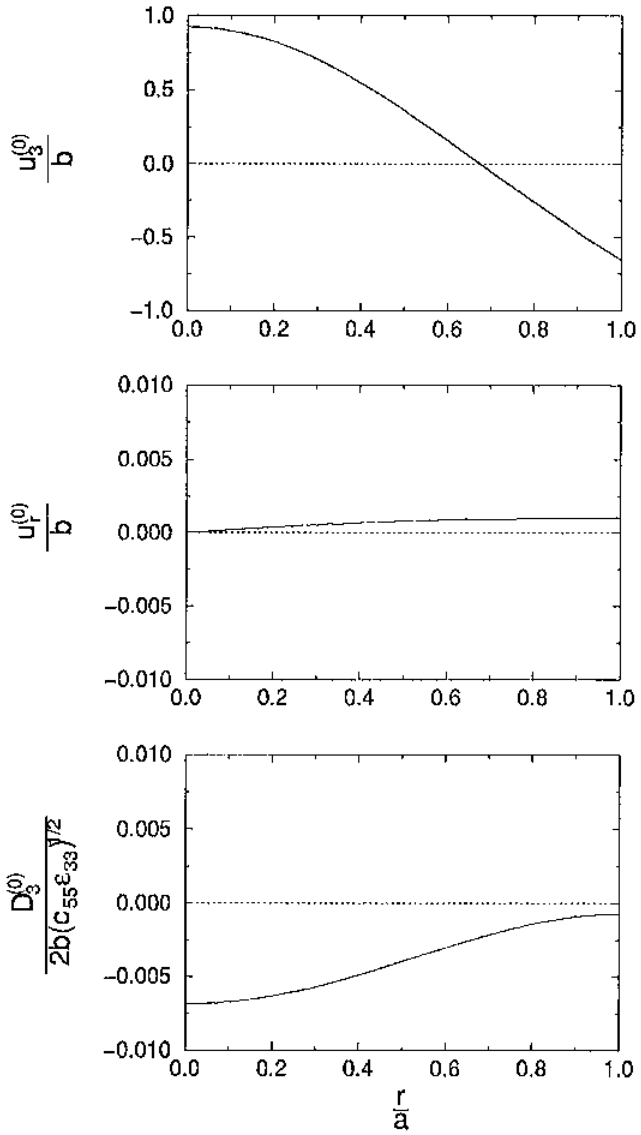

Fig. 4. Distributions of displacements and electric charge of the first mode F_1 (fundamental flexural mode, $f = 11$ kHz) of the asymmetric bimorph disk of PZT-857 with $a = 1.27$ cm, and $b_1 = 0.100$ cm, $b_2 = 0.0127$ cm.

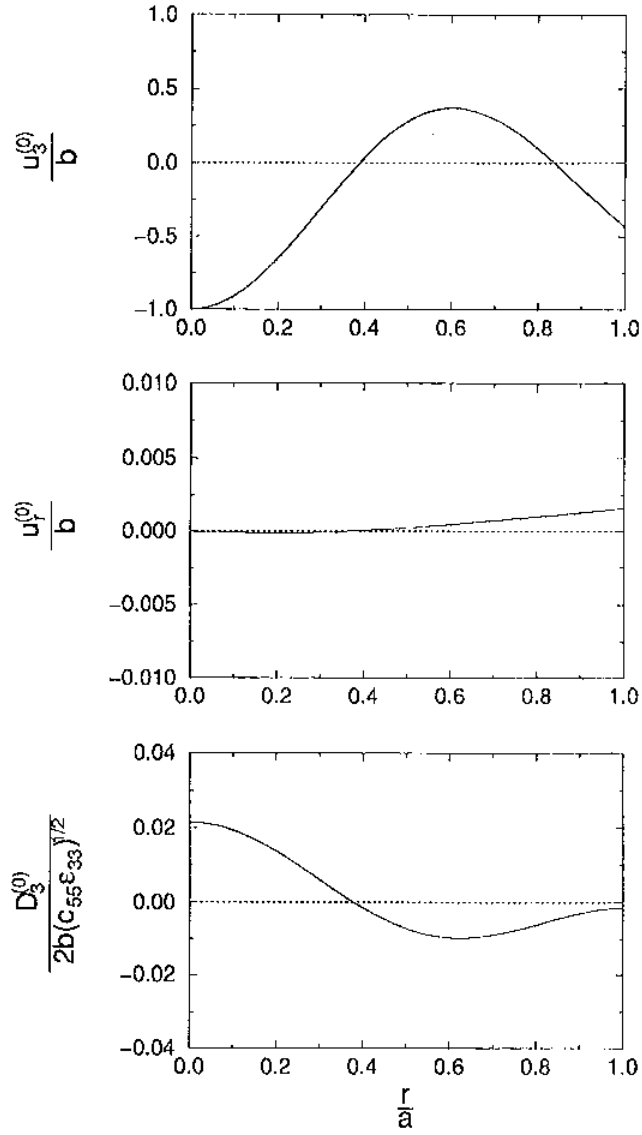

Fig. 5. Distributions of displacements and electric charge of the second mode F_2 (predominantly flexural, $f = 43$ kHz) of the asymmetric bimorph disk of PZT-857 with $a = 1.27$ cm, and $b_1 = 0.100$ cm, $b_2 = 0.0127$ cm.

fundamental radial mode (R_1), respectively, as they are denoted in Fig. 3.

IV. Piezoelectrically Forced Vibrations

Consider an alternating voltage impressed across the electrodes, i.e., $\phi(x_3 = \pm b) = \pm\phi_0 e^{i\omega t}$. According to the series expansion of the electric potential in (3), we have

$$\bar{V}_1 = \phi_0 e^{i\omega t}. \tag{30}$$

To find the particular solution, we assume

$$\begin{aligned} u_3^{(1)} &= \frac{\phi_0}{b}\sqrt{\frac{\varepsilon_{33}}{c_{55}}}G_1 e^{i\omega t}, \\ \phi^{(0)} &= \phi_0 G_2 e^{i\omega t}, \\ \phi^{(1)} &= \frac{\phi_0}{b} G_3 e^{i\omega t}, \\ \nabla\cdot\mathbf{u}_T^{(0)} &= \nabla\cdot\mathbf{u}_T^{(1)} = u_3^{(0)} = 0. \end{aligned} \tag{31}$$

By substituting (31) into (4) and (14) and setting $\mathbf{F}_T^{(0)}, \mathbf{F}_T^{(1)}, \mathcal{F}_3^{(0)}, \mathcal{F}_3^{(1)}$ to zero, we have

$$\sum_{k=1}^{3} Q_{(3+i)(3+k)}(X=0;\Omega)G_k = \Phi_i, \quad i = 1,2,3 \tag{32}$$

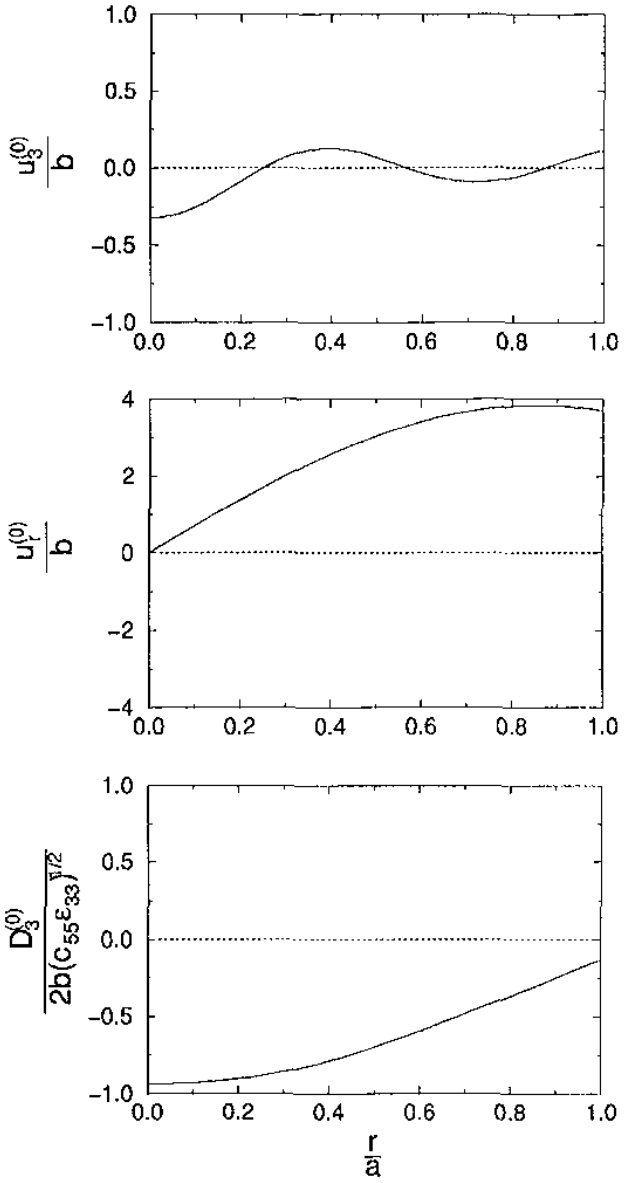

Fig. 6. Distributions of displacements and electric charge of the fourth mode R_1 (fundamental extensional mode, $f = 93$ kHz) of the asymmetric bimorph disk of PZT-857 with $a = 1.27$ cm, and $b_1 = 0.100$ cm, $b_2 = 0.0127$ cm.

where Q_{ij} are given in (17) and

$$\begin{aligned}\Phi_1 &= \frac{\kappa_3 \bar{e}_{33}}{\sqrt{c_{55}\epsilon_{33}}},\\ \Phi_2 &= \frac{2b\bar{e}_{33}^{(1)}}{3\epsilon_{33}},\\ \Phi_3 &= \frac{\bar{e}_{31}^{(0)} - \bar{e}_{33}^{(2)}}{\epsilon_{33}}.\end{aligned} \tag{33}$$

The complete solution consists of particular solution (31) and complementary solution, which is identical to the

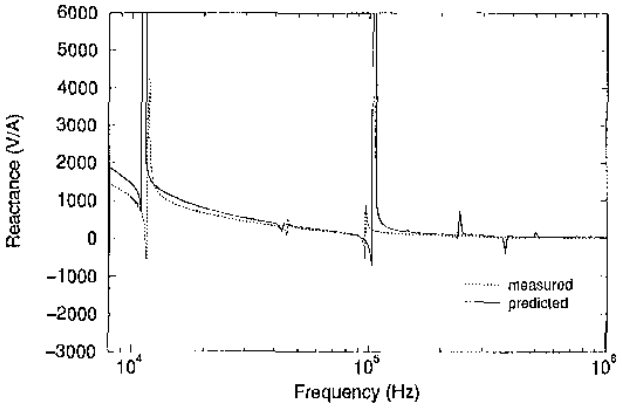

Fig. 7. Comparison of computed reactance (solid line) with the measured values (dotted line) for the asymmetric bimorph disk of PZT-857 with $a = 1.27$ cm, and $b_1 = 0.100$ cm, $b_2 = 0.0127$ cm.

solution (22) for free vibrations. Hence, we have

$$\begin{aligned}\nabla \cdot \mathbf{u}_T^{(0)} &= \sum_{j=1}^{6} \alpha_{1j} B_j J_0(\xi_j r) e^{i\omega t},\\ u_3^{(0)} &= b\sum_{j=1}^{6} \alpha_{2j} B_j J_0(\xi_j r) e^{i\omega t},\\ \nabla \cdot \mathbf{u}_T^{(1)} &= \frac{1}{b}\sum_{j=1}^{6} \alpha_{3j} B_j J_0(\xi_j r) e^{i\omega t},\\ u_3^{(1)} &= \left[\frac{\phi_0}{b}\sqrt{\frac{\epsilon_{33}}{c_{55}}} G_1 + \sum_{j=1}^{6} \alpha_{4j} B_j J_0(\xi_j r)\right] e^{i\omega t},\\ \phi^{(0)} &= \left[\phi_0 G_2 + b\sqrt{\frac{c_{55}}{\epsilon_{33}}}\sum_{j=1}^{6} \alpha_{5j} B_j J_0(\xi_j r)\right] e^{i\omega t},\\ \phi^{(1)} &= \left[\frac{\phi_0}{b} G_3 + \sqrt{\frac{c_{55}}{\epsilon_{33}}}\sum_{j=1}^{6} \alpha_{6j} B_j J_0(\xi_j r)\right] e^{i\omega t}.\end{aligned} \tag{34}$$

We note that the radial components of the displacement in (26) remain the same because the particular solution in (31) is independent of the space variable r. By substituting (34) and (26) into the edge conditions (12), we obtain

$$\sum_{j=1}^{6} M_{ij} B_j' = C_i, \quad i = 1, \cdots, 6 \tag{35}$$

where the coefficients M_{ij} are given in (29) and

$$\begin{aligned}B_j' &= \frac{b}{\phi_0}\sqrt{\frac{c_{55}}{\epsilon_{33}}} B_j, \quad j = 1, \cdots, 6,\\ C_1 &= -\kappa_3 \frac{e_{13}}{c_{55}} G_1 + \frac{2b\bar{e}_{31}^{(1)}}{3\sqrt{c_{55}\epsilon_{33}}} G_2 - \frac{e_{31} - e_{31}^{(0)}}{\sqrt{c_{55}\epsilon_{33}}} G_3 - \frac{\bar{e}_{31}}{\sqrt{c_{55}\epsilon_{33}}},\\ C_2 &= \frac{2\bar{e}_{31}^{(0)}}{\sqrt{c_{55}\epsilon_{33}}} G_2 - \frac{b(\bar{e}_{31}^{(1)} - \frac{2}{5}\bar{e}_{31}^{(3)})}{\sqrt{c_{55}\epsilon_{33}}} G_3 - \frac{b\bar{e}_{31}^{(1)}}{\sqrt{c_{55}\epsilon_{33}}},\\ C_j &= 0, \quad j = 3, \cdots, 6.\end{aligned} \tag{36}$$

We note that B_j' in (35) is independent of the applied voltage ϕ_0 because M_{ij} and C_i are voltage independent. Therefore, from $(36)_1$, we see that B_j is linearly dependent on ϕ_0. Thus, from (34), the complete solution is also linearly dependent on ϕ_0.

The total surface charge on the electroded surfaces of the disk is

$$Q = -\frac{\pi}{b}\int_0^a D_3^{(0)} r dr \tag{37}$$

where $D_3^{(0)}$ is the zero-order 2-D charge density. From the 2-D equation $(83)_3$ of [1], we have

$$D_3^{(0)} = 2b\left[\bar{e}_{31}\nabla\cdot\mathbf{u}_T^{(0)} + \kappa_3\bar{e}_{33}u_3^{(1)} - (\hat{e}_{33}^{(0)} - \hat{e}_{33}^{(2)})\phi^{(1)} - \hat{e}_{33}^{(0)}\frac{\bar{V}_1}{b}\right] + \frac{2b^3}{3}\left[\bar{e}_{31}^{(1)}\nabla\cdot\mathbf{u}_T^{(1)} + \frac{2}{b^2}\hat{e}_{33}^{(1)}\phi^{(0)}\right]. \tag{38}$$

Substitution of the solution (34) into (38), and then into (37) leads to

$$Q = \pi a^2 c_{33}\frac{\bar{\phi}_0}{b}\left[H - 2\sum_{j=1}^{6}\gamma_j B_j'\frac{J_1(\xi_j a)}{\xi_j a}\right]e^{i\omega t} \tag{39}$$

where

$$\begin{aligned}\gamma_j &= \frac{\bar{e}_{31}}{\sqrt{c_{55}\epsilon_{33}}}\alpha_{1j} + \frac{b\bar{e}_{31}^{(1)}}{3\sqrt{c_{55}\epsilon_{33}}}\alpha_{3j} + \frac{\kappa_3\bar{e}_{33}}{\sqrt{c_{55}c_{33}}}\alpha_{4j} + \frac{2b\hat{e}_{33}^{(1)}}{3\epsilon_{33}}\alpha_{5j} - \frac{\hat{e}_{33}^{(0)}-\hat{e}_{33}^{(2)}}{\epsilon_{33}}\alpha_{6j},\\ H &= -\frac{\kappa_3\bar{e}_{33}}{\sqrt{c_{55}c_{33}}}G_1 - \frac{2b\hat{e}_{33}^{(1)}}{3\epsilon_{33}}G_2 + \frac{\hat{e}_{33}^{(0)}-\hat{e}_{33}^{(2)}}{\epsilon_{33}}G_3 + \frac{\hat{e}_{31}^{(0)}}{c_{33}}.\end{aligned} \tag{40}$$

By using $I = \dot{Q}$, we obtain the impedance

$$Z = \frac{2\bar{V}_1}{I} = -i\frac{2b}{\omega\pi a^2 c_{33}}\left[H - 2\sum_{j=1}^{6}\gamma_j B_j'\frac{J_1(\xi_j a)}{\xi_j a}\right]^{-1} \tag{41}$$

and the motional capacitance

$$C = \frac{Q}{2\bar{V}_1} = \epsilon_{33}\frac{\pi a^2}{2b}\left[H - 2\sum_{j=1}^{6}\gamma_j B_j'\frac{J_1(\xi_j a)}{\xi_j a}\right]. \tag{42}$$

We note that the impedance in (41) is purely imaginary because no dissipation is taken into consideration. From (41), we also see the reactance (imaginary part of the impedance) is approximately inversely proportional to the frequency, behaving like a capacitor in electric circuits.

The reactance as a function of forcing frequency is computed from (41) and plotted as the solid line in Fig. 7 for an asymmetric bimorph disk of PZT-857 with $a = 1.27$ cm and $r_t = 0.127$. The measured reactance is also presented in the same figure as the dashed line for comparison. It is seen from Fig. 7 that the predicted result agrees closely with the measurement.

V. Static Responses

In this section, we consider responses under static voltage difference, i.e., when the frequency of the impressed alternating voltage in (30) approaches zero.

From the dispersion curves in Fig. 2, we see that, at $\Omega = 0$, there are three distinct non-zero wave numbers that are denoted by X_1, X_2, and X_3 and a triple zero wave number denoted by $X_4 = 0$.

The complementary solutions corresponding to $X_j, j = 1,2,3$ are the same as those given in (22) and (23), except that $\omega = 0$. The three linearly independent solutions corresponding to the triple root $X_4 = 0$ are given below:

$$\begin{aligned}\nabla\cdot\mathbf{u}_T^{(0)} &= B_4, & 0, \quad & 0,\\ u_3^{(0)} &= 0, & bB_5, \quad & bB_6\left(\tfrac{r}{2b}\right)^2,\\ \nabla\cdot\mathbf{u}_T^{(1)} &= 0, & 0, \quad & -\tfrac{1}{b}B_6,\\ u_3^{(1)} &= \eta_{11}B_4, & 0, \quad & \eta_{12}B_6,\\ \phi^{(0)} &= b\eta_{21}B_4\sqrt{\tfrac{c_{55}}{\epsilon_{33}}}, & 0, \quad & b\eta_{22}B_6\sqrt{\tfrac{c_{55}}{\epsilon_{33}}},\\ \phi^{(1)} &= \eta_{31}B_4\sqrt{\tfrac{c_{55}}{\epsilon_{33}}}, & 0, \quad & \eta_{32}B_6\sqrt{\tfrac{c_{55}}{\epsilon_{33}}}\end{aligned} \tag{43}$$

where $\eta_{kj}, k = 1,2,3; j = 1,2$ satisfy

$$\sum_{k=1}^{3} Q_{(3+i)(3+k)}(X=0;\Omega=0)\eta_{kj} = \mathrm{A}_{ij}, \quad i = 1,2,3 \tag{44}$$

with Q_{ij} given in (17) and

$$[\mathrm{A}_{ij}] = \begin{bmatrix} \kappa_3\frac{c_{13}}{c_{55}} & 0\\ \frac{2b\bar{e}_{31}^{(1)}}{3\sqrt{c_{55}\epsilon_{33}}} & \frac{2\bar{e}_{31}^{(0)}}{3\sqrt{c_{55}c_{33}}}\\ \frac{e_{31}^{(4)}}{\sqrt{c_{55}\epsilon_{33}}} & \frac{b(\kappa_5\bar{e}_{15}^{(5)}-\hat{e}_{31}^{(5)})}{3\sqrt{c_{55}\epsilon_{33}}}\end{bmatrix}. \tag{45}$$

The particular solution for static case is obtained from (31) and (32) by setting $\omega = 0$. Hence, the complete solution for the static response of an asymmetric bimorph disk is

$$\begin{aligned}\nabla\cdot\mathbf{u}_T^{(0)} &= \sum_{j=1}^{3}\alpha_{1j}B_jJ_0(\xi_j r) + B_4,\\ u_3^{(0)} &= b\left[\sum_{j=1}^{3}\alpha_{2j}B_jJ_0(\xi_j r) + B_5 + B_6\left(\frac{r}{2b}\right)^2\right],\\ \nabla\cdot\mathbf{u}_T^{(1)} &= \frac{1}{b}\left(\sum_{j=1}^{3}\alpha_{3j}B_jJ_0(\xi_j r) - B_6\right),\\ u_3^{(1)} &= \frac{\bar{V}_1}{b}\sqrt{\frac{\epsilon_{33}}{c_{55}}}G_1 + \sum_{j=1}^{3}\alpha_{4j}B_jJ_0(\xi_j r) + \eta_{11}B_4 + \eta_{12}B_6,\\ \phi^{(0)} &= \bar{V}_1G_2 + b\sqrt{\frac{c_{55}}{\epsilon_{33}}}\left[\sum_{j=1}^{3}\alpha_{5j}B_jJ_0(\xi_j r) + \eta_{21}B_4 + \eta_{22}B_6\right],\\ \phi^{(1)} &= \frac{V_1}{b}G_3 + \sqrt{\frac{c_{55}}{\epsilon_{33}}}\left[\sum_{j=1}^{3}\alpha_{6j}B_jJ_0(\xi_j r) + \eta_{31}B_4 + \eta_{32}B_6\right],\end{aligned} \tag{46}$$

For axisymmetric deformation, $(46)_{1,3}$ can be integrated easily to obtain $u_r^{(0)}$ and $u_r^{(1)}$:

$$\begin{aligned}u_r^{(0)} &= \sum_{j=1}^{3}\alpha_{1j}B_j\frac{J_1(\xi_j r)}{\xi_j} + \frac{1}{2}B_4 r,\\ u_r^{(1)} &= \frac{1}{b}\left(\sum_{j=1}^{3}\alpha_{3j}B_j\frac{J_1(\xi_j r)}{\xi_j} - \frac{1}{2}B_6 r\right).\end{aligned} \tag{47}$$

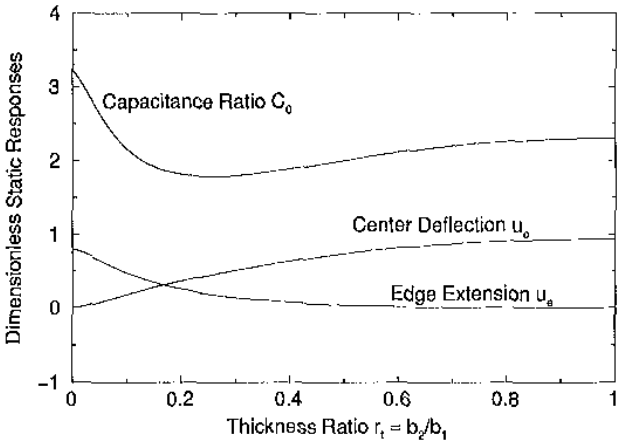

Fig. 8. Effect of thickness ratio r_t on the center deflection $\bar{u}_c$, edge radial displacement $\bar{u}_e$, and capacitance ratio $\bar{C}_0$ of asymmetric bimorph disks of PZT-857 under static voltage difference.

Substitution of (46) and (47) into the free edge conditions (12) results in

$$B_1' = B_2' = B_3' = 0,$$
$$\begin{bmatrix} H_{11} & H_{12} \\ H_{21} & H_{22} \end{bmatrix} \begin{pmatrix} B_4' \\ B_6' \end{pmatrix} = \begin{pmatrix} C_1 \\ C_2 \end{pmatrix} \tag{48}$$

where

$$\begin{aligned} B_j' &= \frac{b}{\bar{V}_1}\sqrt{\frac{c_{55}}{c_{33}}}B_j, \quad j = 1, \cdots, 6, \\ H_{11} &= \frac{c_{11}+c_{12}}{2c_{55}} + \kappa_3\frac{e_{13}}{c_{55}}\eta_{11} - \frac{2b\bar{e}_{31}^{(1)}}{3\sqrt{c_{55}\epsilon_{33}}}\eta_{21} + \frac{\bar{e}_{31}^{(4)}}{\sqrt{c_{55}\epsilon_{33}}}\eta_{31}, \\ H_{12} &= \kappa_3\frac{e_{13}}{c_{55}}\eta_{12} - \frac{2b\bar{e}_{31}^{(1)}}{3\sqrt{c_{55}\epsilon_{33}}}\eta_{22} + \frac{\bar{e}_{31}^{(4)}}{\sqrt{c_{55}\epsilon_{33}}}\eta_{32}, \\ H_{21} &= -\frac{2\bar{e}_{31}^{(0)}}{\sqrt{c_{55}\epsilon_{33}}}\eta_{21} + \frac{b\bar{e}_{31}^{(5)}}{\sqrt{c_{55}\epsilon_{33}}}\eta_{31}, \\ H_{22} &= -\frac{\bar{e}_{11}^{(0)}+\bar{e}_{12}^{(0)}}{2c_{55}} - \frac{2\bar{e}_{31}^{(0)}}{\sqrt{c_{55}\epsilon_{33}}}\eta_{22} + \frac{b\bar{e}_{31}^{(5)}}{\sqrt{c_{55}\epsilon_{33}}}\eta_{32}, \end{aligned} \tag{49}$$

and C_1 and C_2 are defined in (36).

From (48), we see that B_4', and B_6' are independent of $\bar{V}_1$, a and b. Hence, by $(49)_1$, the non-zero amplitudes B_4 and B_6 are linearly dependent on the applied voltage and their dependence on thickness ratio r_t is through the modified piezoelectric coefficients given in (11).

We note that the amplitude B_5 contained in $u_3^{(0)}$ of $(46)_2$ corresponds to a rigid-body displacement of the disk and does not affect the strains or stresses. To compute the transverse displacement $u_3^{(0)}$ at the center of the disk relative to the displacement at the edge, we let $u_3^{(0)}|_{r=a} = 0$, then

$$B_5 = -B_6\left(\frac{a}{2b}\right)^2. \tag{50}$$

Therefore, the center deflection of the disk is

$$u_3^{(0)}|_{r=0} = -\bar{V}_1\frac{a^2}{4b^2}\sqrt{\frac{\epsilon_{33}}{c_{55}}}B_6', \tag{51}$$

and the radial displacement at the edge of the disk is

$$u_r^{(0)}|_{r=a} = \bar{V}_1\frac{a}{2b}\sqrt{\frac{\epsilon_{33}}{c_{55}}}B_4'. \tag{52}$$

From these equations, we see that the center deflection of the bimorph disk is proportional to $(a/b)^2$, and the radial displacement is proportional to a/b; both of them are linearly dependent on the impressed voltage.

The static surface charge density is

$$D_3^{(0)} = 2\bar{V}_1\epsilon_{33}\left[-H + \gamma_1 B_4' + \gamma_2 B_6'\right] \tag{53}$$

where H is the same as that defined in $(40)_2$ and

$$\begin{aligned} \gamma_1 &= \\ &\frac{\bar{e}_{31}}{\sqrt{c_{55}\epsilon_{33}}} + \frac{\kappa_3 e_{33}}{\sqrt{c_{55}\epsilon_{33}}}\eta_{11} + \frac{2b\bar{e}_{33}^{(1)}}{3\epsilon_{33}}\eta_{21} - \frac{\bar{e}_{33}^{(0)}-\bar{e}_{33}^{(2)}}{\epsilon_{33}}\eta_{31}, \\ \gamma_2 &= \\ &-\frac{b\bar{e}_{31}^{(1)}}{3\sqrt{c_{55}\epsilon_{33}}} + \frac{\kappa_3 e_{33}}{\sqrt{c_{55}\epsilon_{33}}}\eta_{12} + \frac{2b\bar{e}_{33}^{(1)}}{3\epsilon_{33}}\eta_{22} - \frac{\bar{e}_{33}^{(0)}-\bar{e}_{33}^{(2)}}{\epsilon_{33}}\eta_{32}. \end{aligned} \tag{54}$$

Substitution of (53) into (37) gives the total surface charge

$$Q = \epsilon_{33}\bar{V}_1\frac{\pi a^2}{b}\left[H - \gamma_1 B_4' - \gamma_2 B_6'\right]. \tag{55}$$

Hence, the motional capacitance as $\omega \to 0$ becomes

$$C_0 = \frac{Q}{2\bar{V}_1} = \epsilon_{33}\frac{\pi a^2}{2b}\left[H - \gamma_1 B_4' - \gamma_2 B_6'\right]. \tag{56}$$

By dividing (51), (52), and (56) by factors $\bar{V}_1\frac{a^2}{4b^2}\sqrt{\frac{c_{33}}{c_{55}}}$, $\bar{V}_1\frac{a}{2b}\sqrt{\frac{c_{33}}{c_{55}}}$, and $\epsilon_{33}\frac{\pi a^2}{2b}$, respectively, we obtain the center deflection $\bar{u}_c$, edge radial displacement $\bar{u}_e$, and capacitance $\bar{C}_0$ in dimensionless form:

$$\bar{u}_c = -B_6', \quad \bar{u}_e = B_4', \quad \bar{C}_0 = H - \gamma_1 B_4' - \gamma_2 B_6'. \tag{57}$$

We note that they are independent of $\bar{V}_1$ and a/b but dependent on $\bar{b}/b$ or $r_t = b_2/b_1$ through (11). The dimensionless quantities in (57) are computed as functions of thickness ratio r_t for asymmetric bimorph disks of PZT-857 and are shown in Fig. 8. It is seen in Fig. 8, $\bar{u}_c$ increases from zero to a maximum, and $\bar{u}_e$ decreases from a maximum to zero, as r_t varies from 0 (for homogeneous plates) to 1 (for symmetric bimorphs). The capacitance $\bar{C}_0$ at $r_t = 1$ is about 70% of the maximum value at $r_t = 0$, and it has a minimum value at $r_t \approx 0.25$, which is about 50% of the maximum value.

VI. Conclusions

Governing equations of coupled flexural and extensional vibrations for asymmetric bimorph plates of piezoelectric ceramics are deduced. Closed-form solutions of these 2-D, first-order equations for circular disks with free edges are obtained for free vibrations, piezoelectrically forced vibrations, and responses induced by static voltage difference.

Resonance frequencies, distributions of displacements and surface charge, impedances, and static responses are computed and examined with the thickness ratio r_t =

$$\begin{bmatrix} -\eta b\sin\eta b - R_c & \eta b\cos\eta b - R_s & 0 & 0 & \hat{e}_{33}^2 & 0 \\ 0 & 0 & \eta b\sin\eta b + R_c & \eta b\cos\eta b - R_s & 0 & \hat{e}_{33}^2 \\ \cos\eta\bar{b} & -\sin\eta\bar{b} & -\cos\eta\bar{b} & \sin\eta\bar{b} & 0 & 0 \\ \cos\eta\bar{b} - \cos\eta b & -\sin\eta\bar{b} + \frac{\bar{b}}{b}\sin\eta b & \cos\eta\bar{b} - \cos\eta b & -\sin\eta\bar{b} + \frac{\bar{b}}{b}\sin\eta b & -\frac{b_1}{b} & \frac{b_2}{b} \\ \eta b\sin\eta\bar{b} & \eta b\cos\eta\bar{b} - \hat{e}_{33}^2\sin\eta b & -\eta b\sin\eta\bar{b} & -\eta b\cos\eta\bar{b} + \hat{e}_{33}^2\sin\eta b & \hat{e}_{33}^2 & -\hat{e}_{33}^2 \\ 0 & \sin\eta b & 0 & \sin\eta b & -1 & -1 \end{bmatrix} \tag{A7}$$

b_2/b_1 and radius-thickness ratio a/b as the varying parameters. Experimental data on resonances and impedances for circular disks of asymmetric bimorph of PZT-857 are obtained. Comparisons of predicted and measured results show that the agreements are close.

Appendix A

Solutions and frequency equations of simple thickness vibrations of an infinite asymmetric bimorph plate of piezoelectric ceramics are obtained from the 3-D equations of linear piezoelectricity in a manner similar to that of [1]. Field equations, surface conditions, and continuity conditions are the same as those in (13)–(16) of [1], except that we consider only the simple modes, i.e.,

$$u_i = u_i(x_3, t), \quad \phi = \phi(x_3, t), \quad i = 1, 2, 3, \tag{A1}$$

and the continuity condition, equation (15) of [1], is required at $x_3 = -\bar{b}$ for asymmetric bimorph plates.

A. Simple Thickness-Shear Modes

Antisymmetric modes:

$$u_1 = A\sin(\eta x_3)e^{i\omega t}, \quad \tan(\eta b) = (R\eta b)^{-1}; \tag{A2}$$

symmetric modes:

$$u_1 = A\cos(\eta x_3)e^{i\omega t}, \quad \tan(\eta b) = -R\eta b \tag{A3}$$

where the frequency $\omega = \eta\sqrt{c_{55}/\rho}$.

B. Simple Thickness-Stretch Modes

$$u_3 = \begin{cases} (A_1\cos\eta x_3 + A_2\sin\eta x_3)e^{i\omega t}, & for\ x_3 > -\bar{b}, \\ (A_3\cos\eta x_3 + A_4\sin\eta x_3)e^{i\omega t}, & for\ x_3 < -\bar{b}, \end{cases}$$

$$\phi = \begin{cases} \frac{e_{33}}{c_{33}}\left[A_1(\cos\eta x_3 - \cos\eta b) + A_2(\sin\eta x_3 - \frac{x_3}{b}\sin\eta b) + A_5(\frac{x_3}{b} - 1)\right]e^{i\omega t}, \\ x_3 > -\bar{b}, \\ -\frac{e_{33}}{c_{33}}\left[A_3(\cos\eta x_3 - \cos\eta b) + A_4(\sin\eta x_3 - \frac{x_3}{b}\sin\eta b) + A_6(\frac{x_3}{b} + 1)\right]e^{i\omega t}, \\ x_3 < -\bar{b} \end{cases} \tag{A4}$$

where

$$\eta^2 = \frac{\rho\omega^2}{\hat{c}_{33}}, \quad \hat{c}_{33} = c_{33} + \frac{e_{33}^2}{c_{33}}. \tag{A5}$$

The frequency equation is

$$\det[Q_{ij}] = 0 \tag{A6}$$

where the matrix $[Q_{ij}]$ is [see (A7) top of page] and

$$R_c = R\eta^2 b^2\cos\eta b, \; R_s = (\hat{e}_{33}^2 + R\eta^2 b^2)\sin\eta b, \; \hat{e}_{33} = \frac{e_{33}}{\sqrt{\hat{c}_{33}c_{33}}}. \tag{A8}$$

We note that, for simple thickness-shear modes, frequency equations $(A2)_2$ and $(A3)_2$ are identical to those for homogeneous plates, and the symmetric and antisymmetric modes are uncoupled. However, for simple thickness-stretch modes, the symmetric and antisymmetric modes are coupled in (A7) for the asymmetric bimorph plates. By setting $\bar{b}$ to ± 1 or 0, it can be reduced to that for homogeneous plates or symmetric bimorph plates, respectively, and for which the symmetric and antisymmetric modes are uncoupled.

References

[1] P.C.Y. Lee and J. D. Yu, "Governing equations for a piezoelectric plate with graded properties across the thickness," *IEEE Trans. Ultrason., Ferroelect., Freq. Contr.*, vol. 45, no. 1, pp. 236–250, 1998.

[2] P.C.Y. Lee and N. H. Lin, "Effect of thickness ratio on the vibrations of an asymmetric bimorph plate of piezoelectric ceramics," in *Proc. 1998 IEEE Int. Freq. Contr. Symp.*, pp. 891–899.

[3] P.C.Y. Lee, J. D. Yu, X. Li, and W.-H. Shih, "Piezoelectric ceramic disks with thickness-graded material properties," *IEEE Trans. Ultrason., Ferroelect., Freq. Contr.*, vol. 46, no. 1, pp. 205–215, 1999.

Rui Huang (S'97) was born in Lu'an, Anhui, China, in 1972. He received his B.S. and M.E. degrees in Applied Mechanics from University of Science and Technology of China (USTC) in 1994 and 1996, respectively. Currently, he is a Ph.D. student in Mechanics, Materials, and Structures program of Civil and Environmental Engineering Department at Princeton University. His research interests include high frequency vibrations of piezoelectric crystals and ceramics, smart materials and structures, sensors, and actuators.